Osmotic pressure of ^{3}He/^{4}He mixtures at the crystallization pressure and at millikelvin temperatures

Anssi Salmela,* Alexander Sebedash, Juho Rysti, Elias Pentti,† and Juha Tuoriniemi
Low Temperature Laboratory, Aalto University, P.O. Box 15100, FI-00076 AALTO, Finland
(Received 3 February 2011; revised manuscript received 25 February 2011; published 11 April 2011)

The difference between the equilibrium concentration of ^{3}He in the solid and liquid phases alters the crystallization pressure of helium mixtures due to osmotic pressure. This effect was determined with high precision at several concentrations from 0.6% to the zero temperature solubility limit of 8.1% by a specific capacitive pressure gauge. Thereby, the osmotic pressure was deduced at 2.53 MPa—the crystallization pressure of pure ^{4}He—and at millikelvin temperatures. The experimental results are compared with numerical calculations for an interacting Fermi liquid using a quasiparticle potential and an effective mass fitted to experimental data.

DOI: 10.1103/PhysRevB.83.134510 PACS number(s): 67.60.G−, 67.85.Lm, 67.85.Pq, 67.80.B−

I. INTRODUCTION

Osmosis is encountered in liquid systems consisting of two or more distinguishable components. Usually, this is considered under circumstances, where a liquid mixture is divided in two parts by a semipermeable barrier through which some, but not all, of the components of the mixture can move. The system tends to an equilibrium state in which the chemical potentials of the mobile components are equal on both sides of the barrier. In closed containers the transfer of particles changes pressure, so that the equilibrium state may sustain both a concentration difference and a pressure difference that drive particles in opposite directions with equal forces. The equilibrium pressure difference, the osmotic pressure, is an important concept because it provides, on one hand, a macroscopic quantity that can be measured experimentally, and on the other hand, it is directly related to the chemical potential, the key parameter in the microscopic thermodynamical description of the liquid.

Osmosis in helium liquids, in the sense described above, can be studied by having a superleak, permeable to superfluid ^{4}He only, between two volumes of liquid helium below the superfluid transition temperature T_λ.[1–6] The other component may then be either the normal fluid fraction of ^{4}He, having reasonable density at temperatures above $\approx$1 K, or dissolved lighter isotope ^{3}He, soluble to some extent in ^{4}He down to arbitrarily low temperatures. In previous work, the osmotic pressure of helium mixtures has been measured directly at a selection of pressures using a superleak between two volumes, one containing the mixture and the other one containing pure ^{4}He, and by observing the pressure difference between these.[3]

In this work we study the osmotic pressure in dilute ^{3}He-^{4}He mixtures at millikelvin temperatures, restricted to the pressure of crystallization of ^{4}He. Preliminary results have been reported in Ref. 7, but here we extend the range of studied concentrations and expand the theoretical considerations. In our experiment we abandoned the superleak filter between the chambers of pure ^{4}He and the dilute mixture, which completely eliminates the possibility of slow migration of ^{3}He through the superleak. Such migration might have become an issue over time, as measurements at the millikelvin regime can take quite a long time, up to several months. To refresh the reference condition back to pure ^{4}He, one would have had to warm up the system to at least 10 K or so. We actually measured the difference in the crystallization pressures of the mixture and reference pure ^{4}He, which were kept separate from each other at a common temperature in a divided cell—see Fig. 1. Instead of a superleak connecting the two volumes, the pressures in the two chambers are related to each other by virtue of both being in equilibrium with pure ^{4}He solid crystals, so that the crystallization pressure difference can be converted into the osmotic pressure. This relationship will be discussed more thoroughly after describing the experimental details.

We may gain information upon the interaction potential between the ^{3}He quasiparticles in the mixture by comparing the experimentally determined and numerically calculated osmotic pressures. The effective two-particle potential significantly influences the zero-temperature limit of the osmotic pressure, whereas its temperature dependence is primarily governed by the effective mass. The measured concentration dependence of the osmotic pressure at zero-temperature limit can thus be used to determine the parameters of the chosen model potential. This will be discussed later, after presenting the measured data.

II. MEASUREMENT OF THE CRYSTALLIZATION PRESSURE

A. Experimental setup

The real experimental cell (volume $8.3 \pm 0.2\,\mathrm{cm}^3$) adapting to the ideal of Fig. 1 is illustrated in detail in Fig. 1 of Ref. 8. The capacitive pressure transducer, whose flexible diaphragm separated the two volumes of the cell, had a resolution of better than 10 mPa at a working pressure of 2.5 MPa.[9,10]

The cell was thermally anchored to the mixing chamber of a dilution refrigerator, whose temperature was measured by a calibrated commercial Ge resistor (above 50 mK), ^{195}Pt NMR (below 100 mK), a Speer carbon resistor (above 10 mK), and a ^{60}Co nuclear orientation thermometer (from 3 to 30 mK). At the most relevant temperature range to this work (5–50 mK), thermometry was performed mainly by a ^{195}Pt NMR thermometer, which was calibrated against the ^{60}Co nuclear orientation primary thermometer with a precision of better than 5%. In addition, the mixture temperature was monitored by a quartz tuning fork immersed in the liquid,[8,11,12] whereas the exact temperature of the pure ^{4}He phase is practically irrelevant at this low range of temperatures. Nevertheless, both liquid phases were thermalized to the body of the cell by pads of sintered silver powder.

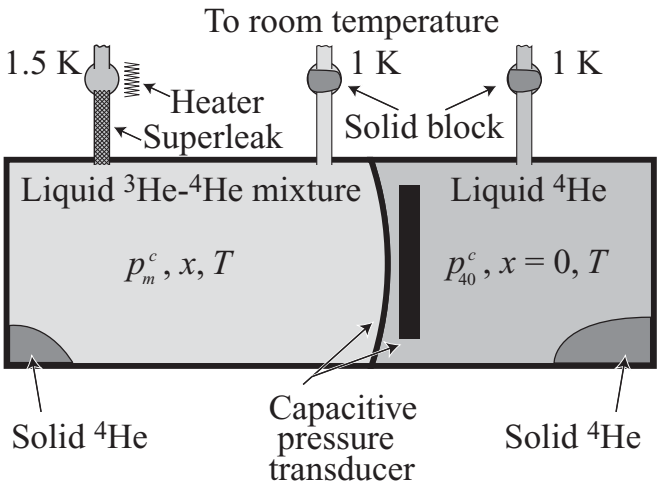

FIG. 1. Schematic illustration of the principle of measuring osmotic pressure of helium mixtures at the crystallization pressure of pure ^{4}He. The filling lines are included since their configuration is essential to the measurement at this high pressure.

The mixtures were prepared by increasing the ^{3}He content in the cell stepwise in a manner explained in Ref. 8. This could be accomplished in one continuous low-temperature run over the entire solubility range by effectively replacing ^{4}He with ^{3}He; ^{4}He was taken out selectively from the cell through a superleak and ^{3}He was inserted through an ordinary capillary. The ^{3}He concentration was determined by careful bookkeeping of the added ^{3}He amounts and verified by means of the quartz tuning fork in the mixture.[8] The stated values are precise to within 0.1% absolute while the relative accuracy is more than an order of magnitude better.[8]

The superleak line connecting to the mixture side of the cell from higher temperature of ∼1.5 K was also used to grow and melt solid ^{4}He into the mixtures. The superleak was needed to bypass the deep minimum in the melting curve of mixtures at ∼1 K temperature. The melting pressure of ^{4}He in the tiny pores of the superleak is considerably higher than that in the bulk liquid. The upper end was kept at a temperature where the bulk melting pressure has already risen sufficiently to avoid blocking at the working pressure but where the superfluid phase still exists, so that transit of ^{4}He in and out through the superleak was always possible in a controlled fashion. The molar flow of ^{4}He through the superleak was measured by a Bronkhorst High-Tech EL-FLOW series mass flow meter at room temperature.

B. Experimental procedure

The measurements progressed from lower to higher concentrations up to the solubility limit in ten consecutive steps. The addition of ^{3}He required lowering the pressure, and since the delicate pressure transducer could not hold pressure differences greater than a few tens of kPa, we had to reduce the pressure on the reference side as well. Therefore, the reference crystal on the pure ^{4}He side had to be prepared again for each new concentration. Once the new mixture was there and the pressure level could be increased again, a small crystal was first grown into the reference volume. To stabilize the reference condition its filling capillary was blocked by another chunk of solid at 1 K or so, created by a fair overpressure to the line, until it was time to change the concentration on the other side again. For each mixture the crystallization pressures were determined at discrete temperatures ranging from 5 to ∼100 mK. That upper value is already so high that some of the simplifying assumptions to be made do not hold anymore, such as the purity with respect to ^{3}He of solid ^{4}He grown into the mixture. Therefore the analysis will be restricted to temperatures lower than 100 mK.

For the given mixture at the chosen temperature, the crystallization pressure was determined according to the scheme described as follows. As transforming part of the liquid mixture into solid pure ^{4}He alters the concentration of the remaining liquid, the size of the solid phase also influences the observed crystallization pressure. Although one might attempt to record the change of concentration in the liquid phase while just growing more solid into the cell and relating the instantaneous concentration and pressure readings, we judged it to be more reliable to determine the crystallization pressure in the limit of a zero-size crystal with a predetermined concentration in the liquid.

This can be accomplished in two obvious ways, although arbitrarily small crystals cannot be created by just increasing the pressure, because there is a considerable nucleation barrier and a corresponding overpressure is needed to make the solid first appear. At the moment of nucleating the solid phase, the overpressure is relaxed by converting an amount of liquid into solid, and one ends up with a crystal of finite size already. Once the conditions have settled after this quite abrupt event, one may grow more solid slowly and observe the increase in pressure as a function of the amount of added helium. This dependence can then be extrapolated backward to the point prior to the nucleation event where the pressure was increased with only liquid in the cell. Since the size of the solid phase and the concentration in the liquid phase increase linearly as a function of added helium, the said extrapolation brings to the point where the solid phase would have been vanishingly small and the concentration would have had the initial liquid-only value. This principle is illustrated in Fig. 2.

There is some uncertainty upon the isotopic purity of the very rapidly grown initial solid. Although the volume of the solid (estimated from the amount of helium added prior to the nucleation) is less than 1% of the total volume of the cell, any appreciable concentration in it would have an observable effect on the melting pressure. Based on our data it is concluded that the concentration of the rapidly grown solid is insignificant for the analysis.

As an alternative to growing, the existing solid can be melted slowly until its disappearance is indicated by an abrupt change in the slope of the pressure versus the amount of helium removed. Such events are also indicated in Fig. 2. The exact pressure of the kink may be influenced by the fact that the curvature of the solid surface slightly alters its melting pressure, becoming more serious as the crystal becomes very small. This effect, however, is apparently insignificant in practice.

Whichever way the size is changed, one must acknowledge that growing or melting the solid in the mixture is associated with a release or absorption of heat. Sufficient periods of relaxation must be allowed after quick changes, otherwise the

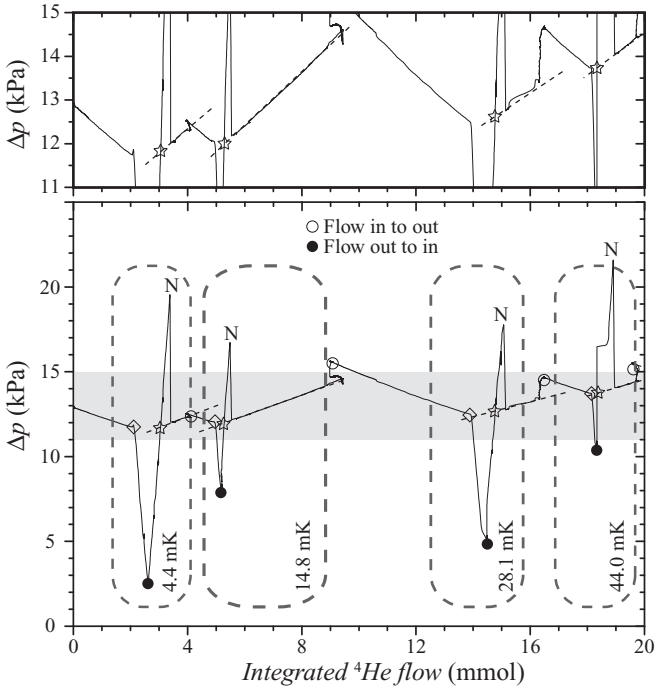

FIG. 2. Pressure difference between a reference crystal in pure ^{4}He and the mixture (3.90% nominal) with or without a solid phase as a function of added or removed ^{4}He, as measured by the integral of the gas flow delivered through the superleak. The direction of the flow in or out has been changed at points indicated by open and filled circles. The nucleation event of each new crystal is marked by the letter "N." The dashed lines fitted to the subsequent slow growth guide the extrapolations of the crystallization pressure to the zero-size crystal, indicated by the star symbols. The diamond symbols indicate the instant of disappearance of the previously grown solid upon slow melting. The temperature had been set in each case to the value shown inside the dashed ovals. There were a couple of hours between each cycle to stabilize the changed temperature but that does not show in the figure, as there obviously was no flow across the superleak during those periods of time. The upper panel displays a closeup of the shaded region in the main frame.

process must be carried out adequately slowly in order not to drift too far out of equilibrium. The two ways, growing or melting, usually produced practically identical values supporting the validity of the method and the unimportance of the obvious nonidealities.

All our measurements of the crystallization pressures at different concentrations and temperatures have been collected in Fig. 3. The data are plotted as a function of the temperature squared, as the leading term in the low-temperature expansion of the quantity of interest is quadratic due to the Fermi statistics of the dilute ^{3}He. This power law is obeyed quite well over the entire range covered, which is not obvious, since the condition of remaining clearly below the Fermi temperature is not always valid, in particular at the lowest concentrations, where the Fermi temperature is rather low already.

III. OSMOTIC PRESSURE AT THE CRYSTALLIZATION PRESSURE

To proceed further on the subject of this paper, we need a method to convert the measured crystallization pressures

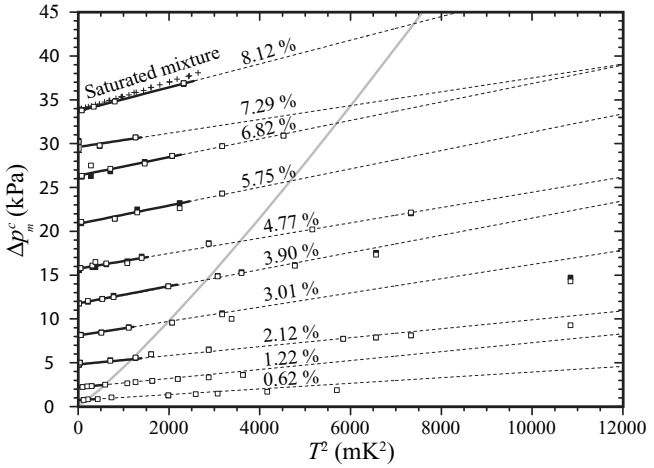

FIG. 3. The change of crystallization pressure, from to 2.53 MPa of pure ^{4}He for different concentrations, as a function of the temperature squared. Crosses indicate measurements in the saturated mixture, whereas the open (solid being melted) and filled (solid being grown) squares indicate measurements below that limit. In most cases such pairs of symbols lie just on top of each other. The black lines show the linear fits to the measured data, and the dashed lines are the extensions of these fits to higher temperatures. The zero-temperature limit of $\Delta p_m^c(T)$ can be found quite accurately from these, whereas obviously there is more scatter in its temperature coefficient $\frac{d\Delta p_m^c(T)}{dT^2}$. The gray line shows the condition $T = T_F/5$.

to values of osmotic pressure. This enables comparison with other measurements performed at lower pressures and also with theory, taking into account the interactions between the ^{3}He quasiparticles in the mixture.

A. Relation between the osmotic and crystallization pressures

The relationship between the two pressures for helium mixtures at low temperatures has been mentioned a couple of times in the literature,[13] but as we have not found any proper derivation for that, we will present it here.

The osmotic pressure π of the helium mixture is the pressure difference relative to pure ^{4}He in thermodynamic equilibrium, that is, when the chemical potentials of ^{4}He in the two phases satisfy the condition

$$\mu_4(p_m, T, x) = \mu_{40}(p_m - \pi, T). \tag{1}$$

Here the subscripts 4 and 40 refer to ^{4}He in the mixture and in the pure phase, respectively, p_m is the pressure of the mixture, and x is the molar fraction of ^{3}He in the mixture. We recall Maxwell's relation for a single-component system,

$$\left(\frac{\partial \mu}{\partial p}\right)_{T,N} = \left(\frac{\partial V}{\partial N}\right)_{p,T}, \tag{2}$$

where the right-hand side is the volume per particle. Then, the change of chemical potential related to a change of pressure can be calculated as

$$\mu(p + \Delta p) = \mu(p) + \int_p^{p+\Delta p} \frac{v(p')}{N_a} dp' = \mu(p) + \frac{\langle v \rangle \Delta p}{N_a}, \tag{3}$$

where $\langle v \rangle$ is the average molar volume in the domain of integration and N_a is the Avogadro constant.

The molar volume of helium mixture is conventionally written as

$$v_m^L = v_{40}^L(1+\alpha x) = v_{40}^L\left(1+\alpha\frac{N_3}{N_3+N_4}\right), \tag{4}$$

where the superscript L refers to the liquid phase and α is an empirical numerical factor that takes into account the larger molar volume of ^{3}He atoms in the mixture.[14] Therefore, the volume of an amount of mixture is

$$\begin{aligned} V &= \frac{(N_3+N_4)}{N_a}v_{40}^L\left(1+\alpha\frac{N_3}{N_3+N_4}\right) \\ &= v_{40}^L\frac{[N_4+(1+\alpha)N_3]}{N_a}, \end{aligned} \tag{5}$$

which implies, omitting the weak concentration dependence of α,[15] that the volume per particle of ^{4}He in the mixture is

$$\left(\frac{\partial V}{\partial N_4}\right) = \frac{v_{40}^L}{N_a}, \tag{6}$$

the same as in the pure phase.

In our case, the two liquid phases are not in equilibrium with each other directly, but instead with separate solids of pure ^{4}He so that their pressures are fixed to the corresponding crystallization pressures p^c. We write the equilibrium condition for them at their individual crystallization pressures:

$$\begin{aligned} \mu_{40}^L(p_{40}^c,T) &= \mu_{40}^S(p_{40}^c,T), \\ \mu_4^L(p_m^c,T,x) &= \mu_4^S(p_m^c,T,0), \end{aligned} \tag{7}$$

where S refers to the solid phase. The solid formed from the liquid mixture is practically pure ^{4}He in the temperature range of interest here.[16] Therefore the chemical potential of the solid in the mixture, μ_4^S, can be calculated at $x=0$. Now, using Eqs. (1), (3), and (6), and denoting $\Delta p^c = p_m^c - p_{40}^c$, we can write the left-hand side of the second equation in (7) as

$$\begin{aligned} \mu_4^L(p_m^c,T,x) &= \mu_{40}^L(p_m^c-\pi,T) = \mu_{40}^L(p_m^c,T) - \frac{\langle v_{40}^L\rangle\pi}{N_a} \\ &= \mu_{40}^L(p_{40}^c+\Delta p^c,T) - \frac{\langle v_{40}^L\rangle\pi}{N_a} \\ &= \mu_{40}^L(p_{40}^c,T) + \frac{\langle v_{40}^L\rangle\Delta p^c}{N_a} - \frac{\langle v_{40}^L\rangle\pi}{N_a}, \end{aligned} \tag{8}$$

and the right-hand side of the same equation as

$$\begin{aligned} \mu_4^S(p_m^c,T,0) &= \mu_{40}^S(p_m^c,T) = \mu_{40}^S(p_{40}^c+\Delta p^c,T) \\ &= \mu_{40}^S(p_{40}^c,T) + \frac{\langle v_{40}^S\rangle\Delta p^c}{N_a}. \end{aligned} \tag{9}$$

The first terms of the resulting forms are equal on the grounds of the first equation in (7) and cancel each other out. We obtain

$$\langle v_{40}^L\rangle\Delta p^c - \langle v_{40}^L\rangle\pi = \langle v_{40}^S\rangle\Delta p^c \Leftrightarrow \pi = \frac{\langle v_{40}^L\rangle - \langle v_{40}^S\rangle}{\langle v_{40}^L\rangle}\Delta p^c, \tag{10}$$

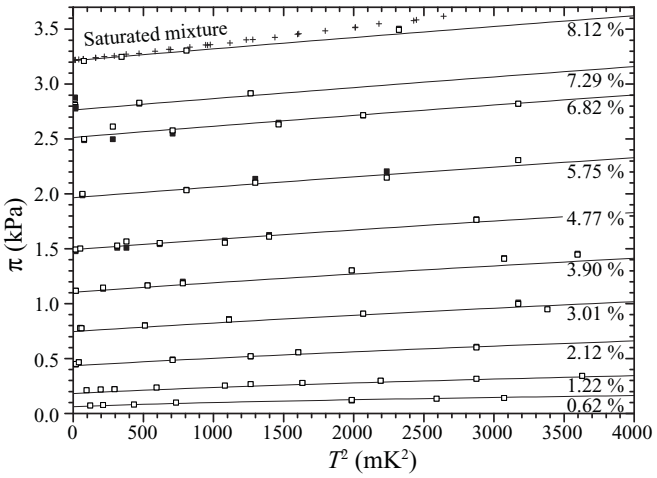

FIG. 4. Osmotic pressure of helium mixtures at 2.53 MPa as a function of temperature squared. The symbols represent the measured values as follows: crosses for the saturated mixture; open and filled squares (on top of each other in many cases) for unsaturated mixtures corresponding to the measurements on melting or growing solid, respectively. The lines are the computed osmotic pressures for the given concentrations using the interaction potential to be discussed in the text.

which is the desired conversion between the osmotic pressure and the pressure difference measured by us.

To evaluate the numerical proportionality factor, average molar volumes can be approximated by those at 2.53 MPa, the melting pressure of pure ^{4}He. The resulting error will be less than 0.1% because of the very small variation of molar volumes within the relevant range of pressures. Applying the values $v_{40}^L = 23.195$ cm^3/mol (Ref. 17) and $v_{40}^S = 20.992$ cm^3/mol,[18] the conversion formula becomes

$$\pi = 0.095\Delta p^c. \tag{11}$$

The data according to this scaling are presented in Fig. 4, together with theoretical curves to be discussed in the next section.

IV. CALCULATION OF OSMOTIC PRESSURE

The difference in chemical potentials of ^{4}He in the mixture and in pure ^{4}He, as in Eq. (8),

$$\Delta\mu_4 = \mu_4(p,T,x) - \mu_{40}(p,T), \tag{12}$$

is related to the osmotic pressure,

$$\pi = -N_a\frac{\Delta\mu_4}{\langle v_{40}\rangle}. \tag{13}$$

We are then left with the task to evaluate the chemical potential difference from the microscopic standpoint. The constraint given by the Gibbs-Duhem relation,

$$\sum_i N_i d\mu_i = -SdT + Vdp, \tag{14}$$

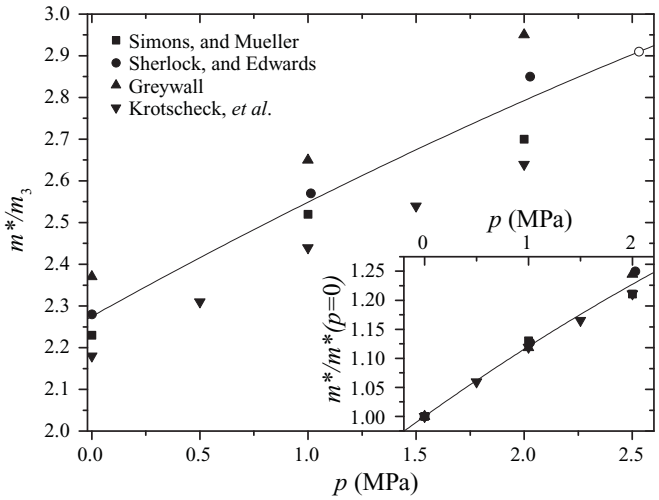

FIG. 5. The pressure dependence of the effective mass of ^{3}He in helium mixtures. The data for various pressures, shown as filled symbols, are taken from Refs. 20–23, while our measurement at the crystallization pressure is shown as the open symbol. The line displays a second-order polynomial fit $m^*/m_3 = 2.276(1 + 0.127\ \mathrm{MPa}^{-1}\,p - 6.618 \times 10^{-3}\ \mathrm{MPa}^{-2}\,p^2)$. The same data sets, scaled by the zero pressure effective mass of each set, respectively, are shown in the inset.

becomes particularly simple when treating the situation at constant temperature T and pressure p, viz., $\sum_i N_i d\mu_i = 0$. For helium mixtures under such circumstances this yields

$$N_3 d\mu_3 + N_4 d\mu_4 = 0 \Rightarrow d\mu_4 = -\frac{N_3}{N_4} d\mu_3 = -\frac{n_3}{n_4}\left(\frac{\partial \mu_3}{\partial n_3}\right)_{T,p} dn_3, \tag{15}$$

where the atom densities n_i may be used instead of the number of atoms N_i. The desired chemical potential difference is obtained by integrating from $n_3 = 0$ in the pure phase to $n_3 = n_3' > 0$ in the mixture (omitting the weak concentration dependence of α):

$$\Delta\mu_4 = \int_0^{n_3'} d\mu_4 = -\int_0^{n_3'} \frac{n_3}{n_4}\left(\frac{\partial \mu_3}{\partial n_3}\right) dn_3 = -\frac{n_3'}{n_{40} - (1+\alpha) n_3'}\mu_3(n_3') + \int_0^{n_3'} \frac{n_{40}}{(n_{40} - (1+\alpha) n_3)^2}\mu_3(n_3) dn_3. \tag{16}$$

It is important to realize that to keep pressure constant, n_4 must depend on n_3 according to $n_4 = n_{40} - (1 + \alpha)n_3$, which is a consequence of Eq. (5). Now, we still need to evaluate μ_3, which will be discussed next.

A. Chemical potential of ^{3}He in the mixture

The chemical potential of ^{3}He in the mixture can be viewed as that of an ideal Fermi gas with an enhanced effective mass plus additional terms due to the quasiparticle interactions. The distribution function for each spin orientation is

$$n(k) = \frac{1}{e^{\beta[\varepsilon(k) - \mu]} + 1}, \tag{17}$$

with quasiparticle energy $\varepsilon(k)$ depending on the wave vector k (momentum $\hbar k$). Here $\beta = 1/k_B T$, and the chemical potential takes a value satisfying the condition

$$n_3 = 2\int n(k)\frac{d^3k}{(2\pi)^3}. \tag{18}$$

The numerical solution of this gives the chemical potential at any concentration and temperature as long as the quasiparticle energy $\varepsilon(k)$ is known.

The contribution of the two particle interactions to the ^{3}He quasiparticle energy, according to the Hartree-Fock approximation, is included in

$$\varepsilon(k) = -E_0 + \frac{\hbar^2 k^2}{2m^*}(1 + \gamma k^2) + n_3 V(0) - \int \frac{d^3k'}{(2\pi)^3} V(\mathbf{k} - \mathbf{k}') n(k'), \tag{19}$$

where the effective quasiparticle interaction potential $V(\mathbf{r})$ has been expressed through its Fourier transform $V(\mathbf{k})$ in momentum space as

$$V(\mathbf{k}) = \int d^3 r e^{-i\mathbf{k}\cdot\mathbf{r}} V(\mathbf{r}). \tag{20}$$

Above, E_0 is the binding energy of a single stationary ^{3}He atom in superfluid ^{4}He and m^* is its effective mass in the zero concentration limit. Actually, E_0 does not contribute to the osmotic pressure, as only the derivative of the chemical potential with respect to the particle density matters. The term $\gamma\hbar^2 k^4/2m^*$ gives a correction at larger values of quasiparticle momenta to the simple effective-mass model of ^{3}He interacting with the background ^{4}He. This is practically insignificant here but is included for completeness. We use the value $\gamma = -0.076$ Å^2 given by Owers-Bradley *et al.*[19]

To construct a viable effective interaction potential $V(\mathbf{k})$ we utilized the zero-temperature osmotic pressure data, presented here, and previously published saturation solubility data.[8] More detailed considerations related to the interaction potential will be published separately.

B. Effective mass

The effective mass of ^{3}He in helium mixtures at the crystallization pressure has not been measured previously. Our osmotic pressure data can be used for this purpose. The main factor determining the temperature dependence of the osmotic pressure at low temperatures is the effective mass, whereas the overall contribution of the interaction potential is less than 10% even at the largest concentration. We analyzed this by treating our data in terms of an ideal Fermi gas and taking the interaction correction into account in an approximate fashion. After iteratively refining the influence of the interaction potential on the temperature dependence, we get $m^* = 2.91 m_3$ at 2.53 MPa pressure. The pressure dependence of the effective mass is reasonably well established[20–23] and our value is consistent with $m^* = 2.28 m_3$ at zero pressure—see Fig. 5.

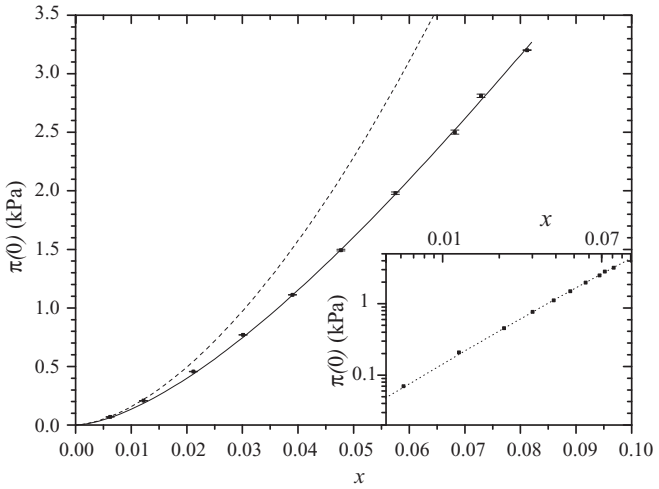

FIG. 6. Osmotic pressure at zero temperature as a function of concentration. The symbols with error bars are the extrapolated values of the experimental data, the error estimates including only the statistical uncertainty in the linear fits. The solid line is the result of the theoretical calculation, while the dashed line represents the behavior if the quasiparticle interactions are omitted. The inset shows the data on logarithmic scales. The dotted line corresponds to a semiempirical fit discussed in the text.

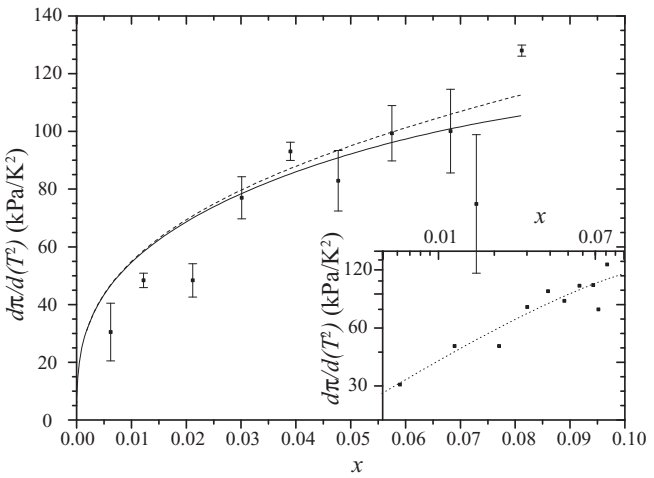

FIG. 7. Coefficient of the quadratic temperature dependence of the osmotic pressure as a function of concentration. The symbols with the error bars are the fitted values to the experimental data, the error estimates including only the inaccuracy of the linear fits. The solid line is the result of the theoretical calculation, while the dashed line represents the behavior if the quasiparticle interactions are omitted. In the inset the data are shown on logarithmic scales with a semiempirical fit described in the text.

This corresponds well with both the experimental values and theory.[24]

V. CONCENTRATION DEPENDENCES

To conclude the description of the measurements and the theoretical analysis, we examine the concentration dependences of the zero-temperature limit of the osmotic pressure as well as its first temperature coefficient at 2.53 MPa. The former is plotted in Fig. 6. The experimental points are the extrapolations to zero temperature of the linear fits to the data on the quadratic temperature axis.

The theoretical curve can be elaborated easily, as the chemical potential becomes the quasiparticle energy at the Fermi wave vector and the distribution function reduces to a simple step function. One then obtains

$$\mu_3 + E_0 = \frac{(\hbar k_F)^2}{2m^*}\left(1 + \gamma k_F^2\right) + n_3 V(0) - \frac{1}{2} n_3 |V(0)| F, \tag{21}$$

with

$$F = \frac{3}{2k_F^3}\int_0^{2k_F} k^2 \left(1 - \frac{k}{2k_F}\right)\frac{V(k)}{|V(0)|}dk. \tag{22}$$

The values for the osmotic pressure can be worked out by integration of (16) and substitution to (13).

It is also possible to work out an expansion of practical value as in Ref. 25. Using the suggested power-law dependences we obtain a fit

$$\pi(0) = 415\ \text{kPa}\left(\frac{x}{1+\alpha x}\right)^{5/3} - 505\ \text{kPa}\left(\frac{x}{1+\alpha x}\right)^{2} - 244\ \text{kPa}\left(\frac{x}{1+\alpha x}\right)^{8/3}, \tag{23}$$

displayed in the inset of Fig. 6. The value of $\alpha = 0.170$ has been used in here, disregarding its weak concentration and temperature dependences. The more elaborate description above incorporated these also.

As seen in Fig. 6, the quasiparticle interactions do modify the predicted dependence quite notably from the corresponding free fermion values, and, therefore, the presented relationship does indeed provide valuable information about the interaction.

The temperature coefficient of the T^2 fits to the experimental data and the theoretical curves are shown in Fig. 7. The theoretical expression corresponds to the asymptotic slopes at $T = 0$ of the calculated curves in Fig. 4. It is worth emphasizing again that the interactions do not significantly influence the first temperature coefficient of the osmotic pressure, but the effective mass does. This is because the effect of the interactions is independent of temperature until the distribution function begins to change significantly at temperatures approaching the Fermi temperature. The semiempirical fit shown in the inset of Fig. 7 is based on a series expansion of Fermi momentum. Again, using $\alpha = 0.170$ we obtain

$$\frac{d\pi}{dT^2} = 10\ \text{kPa/K}^2\left(\frac{x}{1+\alpha x}\right)^{1/3} + 1110\ \text{kPa/K}^2\left(\frac{x}{1+\alpha x}\right)^{2/3} - 1270\ \text{kPa/K}^2\left(\frac{x}{1+\alpha x}\right). \tag{24}$$

Now it is possible to interpolate the data measured at 2.53 MPa to any value of concentration for comparison with other measurements performed at lower pressures. A natural choice for such a comparison is the limiting solubility at the saturated vapor pressure, for which we take $x = 0.0665$. Our data give

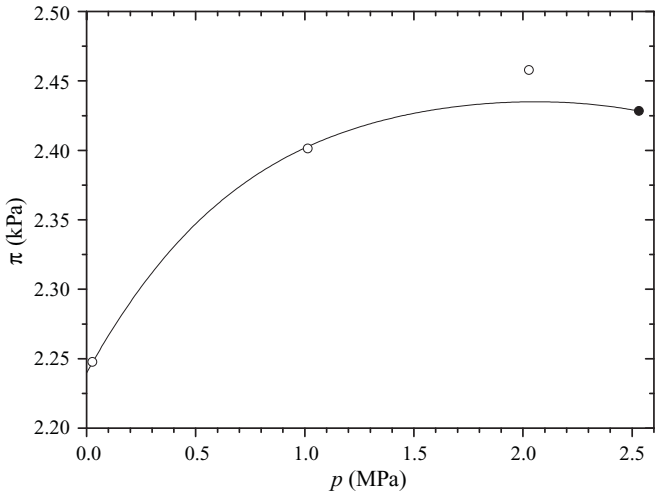

FIG. 8. Osmotic pressure with $x = 0.0665$ at the zero-temperature limit as a function of pressure. Our measurement is displayed as the solid symbol, while the rest of the points are derived from the measurements by Landau *et al*. (Ref. 3). The solid line is a theoretical curve calculated numerically using our interaction potential.

$\pi = 2.43$ kPa, which are displayed in Fig. 8, together with the data from Landau *et al*.[3]

VI. CONCLUSIONS AND DISCUSSION

Osmotic pressures of helium mixtures with concentrations ranging from below 1% to the saturation limit were measured against a reference of pure ^{4}He at the crystallization pressure at millikelvin temperatures. The cell pressure was controlled through a superleak, making it possible to grow solid ^{4}He into the mixture over the entire range of concentration and temperature studied. The results were compared with numerical calculations for interacting Fermi liquid. To determine a proper interaction potential for the calculation, we also resorted to an independent measurement on the solubility of ^{3}He in ^{4}He. Good agreement was found using a credible form for the interaction potential.

Once the interaction potential is determined, one can compute basically any thermodynamic property of the mixture, including the critical temperature of the anticipated superfluid transition in the dilute system. The proposed potential prefers p-wave pairing at high pressures with a T_c of $\sim 20\mu$K at the melting pressure and the maximum concentration. This is obviously out of the reach of methods based on external refrigeration of helium mixtures due to enormous Kapitza resistance at such low temperatures. It is becoming evident that the only way of reaching sufficiently low temperatures for observing the transition to the superfluid state in dilute mixtures is to use processes absorbing heat inherently within the mixture. To be more specific, it should be plausible to perform dilution cooling of the mixture to well below 0.1 mK, perhaps even to the lower microkelvin range by the method of adiabatic melting of solid ^{4}He in presence of superfluid ^{3}He.[26–28] This method operates at the crystallization pressure, giving good motivation to study the thermodynamic properties of mixtures in those particular conditions.

ACKNOWLEDGMENTS

This research was funded by Academy of Finland and by European Community–Research Infrastructures under the FP7 Capacities Specific Programme, MICROKELVIN project No. 228464. Support by Vaisala Foundation and Finnish Cultural Foundation is appreciated. We thank S. Boldarev for valuable technical contributions and S. Burmistrov for discussions and comments.

*ajsalmel@cc.hut.fi
†Present address: Pöyry Finland Oy, P.O. Box 50, Jaakonkatu 2, FI-01621 Vantaa, Finland.

[1] P.-J. Nacher and E. Stoltz, J. Low Temp. Phys. **110**, 281 (1998).
[2] J. Landau, J. T. Tough, N. R. Brubaker, and D. O. Edwards, Phys. Rev. Lett. **23**, 283 (1969).
[3] J. Landau, J. T. Tough, N. R. Brubaker, and D. O. Edwards, Phys. Rev. A **2**, 2472 (1970).
[4] H. London, G. R. Clarke, and E. Mendoza, Phys. Rev. **128**, 1992 (1962).
[5] D. O. Edwards and M. S. Pettersen, J. Low Temp. Phys. **87**, 473 (1992).
[6] M. F. Wilson, D. O. Edwards, and J. T. Tough, Phys. Rev. Lett. **19**, 1368 (1967).
[7] A. P. Sebedash, J. T. Tuoriniemi, E. M. Pentti, and A. J. Salmela, J. Low Temp. Phys. **150**, 181 (2008).
[8] E. M. Pentti, J. T. Tuoriniemi, A. J. Salmela, and A. P. Sebedash, Phys. Rev. B **78**, 064509 (2008).
[9] A. Sebedash, J. T. Tuoriniemi, S. Boldarev, E. M. Pentti, and A. J. Salmela, AIP Conf. Proc. **850**, 1591 (2006).
[10] A. Sebedash, J. Tuoriniemi, E. Pentti, and A. Salmela, J. Phys. Conf. Ser. **150**, 012043 (2009).
[11] D. O. Clubb, O. V. L. Buu, R. M. Bowley, R. Nyman, and J. R. Owers-Bradley, J. Low Temp. Phys. **136**, 1 (2004).
[12] R. Blaauwgeers, M. Blazkova, M. Clovecko, V. Eltsov, R. de Graaf, J. Hosio, M. Krusius, D. Schmoranzer, W. Schoepe, L. Skrbek, P. Skyba, R. Solntsev, and D. Zmeev, J. Low Temp. Phys. **146**, 537 (2007).
[13] B. Castaing, A. S. Greenberg, and M. Papoulat, J. Low Temp. Phys. **47**, 191 (1982).
[14] J. Bardeen, G. Baym, and D. Pines, Phys. Rev. **156**, 207 (1967).
[15] K. Hatakeyama, S. Noma, E. Tanaka, S. N. Burmistrov, and T. Satoh, Phys. Rev. B **67**, 094503 (2003).
[16] D. O. Edwards and S. Balibar, Phys. Rev. B **39**, 4083 (1989).
[17] E. Tanaka, K. Hatakeyama, S. Noma, and T. Satoh, Cryogenics **40**, 365 (2000).
[18] A. Driessen, E. van der Poll, and I. F. Silvera, Phys. Rev. B **33**, 3269 (1986).
[19] J. R. Owers-Bradley, P. C. Main, R. M. Bowley, G. J. Batey, and R. J. Church, J. Low Temp. Phys. **72**, 201 (1988).

[20]R. A. Sherlock and D. O. Edwards, Phys. Rev. A **8**, 2744 (1973).
[21]D. S. Greywall, Phys. Rev. B **20**, 2643 (1979).
[22]R. Simons and R. M. Mueller, Czech. J. Phys. **46**, 201 (1996).
[23]E. Krotscheck, M. Saarela, K. Schörkhuber, and R. Zillich, Phys. Rev. Lett. **80**, 4709 (1998).
[24]M. Boninsegni and D. M. Ceperley, Phys. Rev. Lett. **74**, 2288 (1995).
[25]J. G. M. Kuerten, C. A. M. Castelijns, A. T. A. M. de Waele, and H. M. Gijsman, Cryogenics **25**, 419 (1985).
[26]A. P. Sebedash, Physica B: Condensed Matter **284-288**, 325 (2000).
[27]J. Tuoriniemi, J. Martikainen, E. Pentti, A. Sebedash, S. Boldarev, and G. Pickett, J. Low Temp. Phys. **129**, 531 (2002).
[28]A. P. Sebedash, J. T. Tuoriniemi, S. T. Boldarev, E. M. M. Pentti, and A. J. Salmela, J. Low Temp. Phys. **148**, 725 (2007).